

Fractal internal wave patterns in a tilted square

Stefan Kopecz

March 24, 2006

This report was written during my practical training at Centrum voor Wiskunde en Informatica (CWI) in cooperation with Nederlands Instituut voor Onderzoek der Zee (NIOZ), which was part of my master studies at Universität Kassel. During my time at Amsterdam and Texel I was supervised by Jason E. Frank (CWI) and Leo R. M. Maas (NIOZ).

Complimentary MATLAB files, which I programmed in order to obtain the results presented in this report, can be downloaded from <http://www.nioz.nl>.

This report is about solving the Poincaré equation within a tilted square. This will be done using a ray-tracing method after having prescribed the solution on appropriate parts of the square's boundary. Thereby the difficulty is to locate proper intervals at which the solution can be prescribed. In order to find such intervals it is necessary to study the limit behavior of reflecting characteristics.

1 Introduction

The equation we want to study, the so-called two dimensional Poincaré equation,

$$\frac{\partial^2 \psi}{\partial x^2} - \lambda^2 \frac{\partial^2 \psi}{\partial z^2} = 0 \quad (1)$$

is closely connected to internal waves in a uniformly-stratified, inviscid, linear, hydrostatic, non-rotating, two dimensional Boussinesq fluid. Starting with their governing equations

$$\begin{aligned} \frac{\partial u}{\partial t} &= -\frac{1}{\rho_*} \frac{\partial p}{\partial x}, \\ \frac{1}{\rho_*} \frac{\partial p}{\partial z} &= b := -g \frac{\rho}{\rho_*}, \\ 0 &= \frac{\partial b}{\partial t} + w N^2, \\ 0 &= \frac{\partial u}{\partial x} + \frac{\partial w}{\partial z}, \end{aligned}$$

and introducing a streamfunction $\Psi(x, z, t)$ with $u = -\partial\Psi/\partial z$ and $w = \partial\Psi/\partial x$, which for monochromatic waves of frequency ω becomes

$$\Psi(x, z, t) = \psi(x, z)e^{-i\omega t},$$

the Poincaré equation (1) can be derived, where $\lambda^2 = \omega^2/N^2$, if $\lambda \ll 1$. Thereby t denotes time, u and w are the velocity components in horizontal (x) and vertical (z) direction and g denotes gravity. N is the Brunt-Väisälä frequency, defined by $N^2(z) = -(g/\rho_*)(d\rho_0/dz)$. Buoyancy is given by b , p denotes pressure and ρ as well as ρ_* and ρ_0 are components of the density field. The approach we will use to solve the equation, a ray-tracing method, as well as the derivation of the Poincaré equation is presented in detail in [1].

It is well known that solutions of (1) are given by

$$\psi(x, z) = f(x - \gamma z) - g(x + \gamma z)$$

with arbitrary functions f and g , where $\gamma = \lambda^{-1}$. For future convenience we define

$$\begin{aligned} F(x, z) &= f(x - \gamma z), \\ G(x, z) &= g(x + \gamma z). \end{aligned}$$

We want to solve (1) within a tilted square S , where the boundary condition is given by

$$\psi = 0 \text{ at } \partial S. \quad (2)$$

Applying the boundary condition (2) to a point $(x_0, z_0) \in \partial S$ yields

$$F(x_0, z_0) = G(x_0, z_0). \quad (3)$$

Let (x_1, z_1) be the intersection point of the boundary with the characteristic $c = x - \gamma z$ starting at (x_0, z_0) and (x_2, z_2) the boundary intersection point with the characteristic $d = x + \gamma z$ starting at (x_1, z_1) . Since f remains unchanged along c and $(x_1, z_1) \in \partial S$

$$F(x_0, z_0) = F(x_1, z_1) = G(x_1, z_1),$$

in the same manner g is unchanged along d , which yields

$$G(x_1, z_1) = G(x_2, z_2) = F(x_2, z_2).$$

We see that F and G remain unchanged at the boundary intersections of reflecting characteristics. Thus, we can compute the streamfunction value $\psi(x_0, y_0)$ for any given point (x_0, z_0) by following the characteristics passing through this point until they intersect the boundary on intervals where the function $F = G$ has been prescribed. Thereby the problem is to find appropriate distinct intervals where this function can be prescribed and thus to avoid the ill-posedness of the problem. Therefore it is necessary to study the limit behavior of the reflecting characteristics.

2 Characteristics movement

2.1 Introduction and definitions

As our domain we consider the square $[0, 1] \times [0, 1] \in \mathbb{R}^2$ tilted counterclockwise with tilt angle $0 < \theta < \frac{\pi}{2}$. The angle between the characteristic with positive slope and the vertical will be referred to as ϕ , i. e. $\lambda = \tan(\pi/2 - \phi)$. Thus the angle determining the negative-slope characteristic measured from the vertical is $-\phi$. For the sake of simplicity we switch to a coordinate system parallel to the square's boundaries. From this point of view, we can choose two arbitrary angles ϕ_1 and ϕ_2 determining the slopes of the two characteristics as shown in Figure 1. In the following we consider ϕ_1 to be measured clockwise from the vertical and ϕ_2 to be measured counterclockwise from the vertical. Then θ and ϕ are given by

$$\theta = \frac{\phi_1 - \phi_2}{2}, \quad \phi = \frac{\phi_1 + \phi_2}{2}.$$

It is clear that our initial situation can always be reobtained by rotation.

Furthermore we need some definitions. A characteristic coming from one of the square's corners will be referred to as *critical characteristic*. This denotation will become clearer

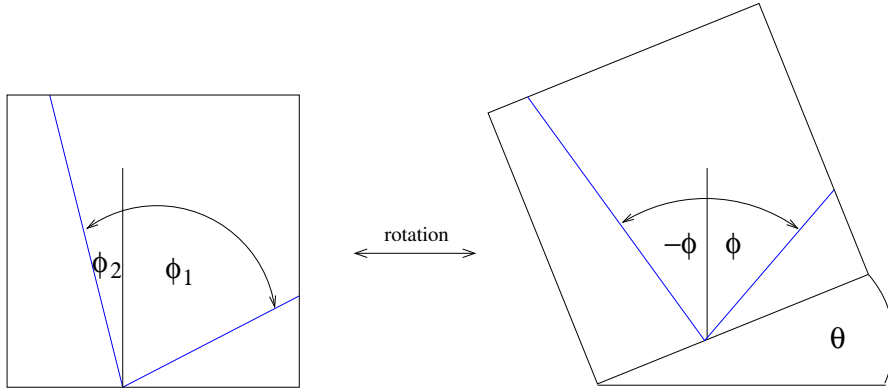


Figure 1: Given two arbitrary angles ϕ_1, ϕ_2 which determine the slopes of the characteristics we can always reobtain the initial situation by rotating the square.

later, when we have a look at the characteristic's movement. The sequence of intersection points with the boundary for a starting point x_0 together with the connecting characteristics will be referred to as the *web* of x_0 and denoted by $S(x_0) = \{\dots, x_{-2}, x_{-1}, x_0, x_1, x_2, \dots\}$, $x_i \in \partial S$.

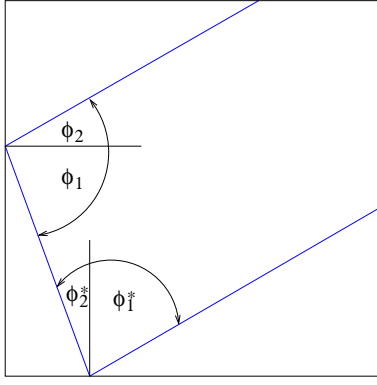
In principle we could choose $-\frac{\pi}{2} \leq \phi_1, \phi_2 \leq \frac{\pi}{2}$, but it is possible to restrict the parameterspace. Without loss of generality, we can take $0 \leq \phi_1$ and $0 \leq |\phi_2| \leq \phi_1$. Otherwise we can get this situation by swapping ϕ_1 and ϕ_2 and or reflecting about the z-axis. If $\phi_1 = \phi_2$, then $\theta = 0$ what has been excluded before. If $\phi_1 = 0$ or $\phi_2 = 0$ one of the characteristics is parallel to the boundary, which yields exceptional reflection behavior. Thus we take strict inequalities. Furthermore, we can assume $\phi_1 \pm \phi_2 \leq \frac{\pi}{2}$. This situation can always be obtained by rotating the domain by $k\pi/2$ for integer k . See figure 2(a). The restricted parameterspace is depicted in figure 2(b).

2.2 Limit behavior

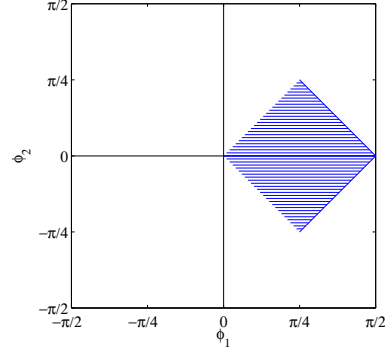
Now we will have a closer look at the characteristic's movement. As we will see there are two different main types of limit behavior depending on whether ϕ_2 is positive or negative. For the following it is convenient to define $t_1 = \tan(\phi_1)$ and $t_2 = \tan(\phi_2)$.

Theorem 1. *For any $\phi_2 < 0$ and for any starting point the characteristics approach to the square's upper left or lower right corner.*

Proof. First of all we can assume the starting point to be at the bottom. In addition we also assume that we trace the characteristics starting with the characteristic determined by ϕ_1 . Let x^* be the x -coordinate of the bottom point which gets mapped directly to the upper right corner, then $x^* = 1 - t_1$ and the sequence of successive bottom intersections



(a) In cases where $\phi_1 + \phi_2 > \frac{\pi}{2}$ we can obtain situation where $\phi_1^* + \phi_2^* < \frac{\pi}{2}$ by rotating the square.



(b) The plot shows the restricted parameterspace. Notice that only those borders which are indicated by a closed line are parts of the parameterspace.

Figure 2:

is given by

$$x_{n+1} = \begin{cases} x_n + t_1 + t_2, & x_n \leq x^*, \\ 1 - (x_n - 1)t_2/t_1, & x^* < x_n. \end{cases}$$

Since $-\phi_1 < \phi_2 < 0$ we have $0 < t_1 + t_2$ and hence $x_n < x_{n+1}$ for $x_n \leq x^*$. We also observe that for any starting point $x_0 \leq x^*$ there exists a $k \in \mathbb{N}$ such that $x^* < x_k$ holds true. For $x_n = 1$ also $x_{n+1} = 1$, thus there is nothing left to prove. For $x^* < x_n < 1$ we have

$$\begin{aligned} x_{n+1} - x_n &= 1 + t_2/t_1 - (t_2/t_1)x_n - x_n \\ &= (1 - x_n)(t_2/t_1 + 1) < 0, \end{aligned}$$

since $x_n < 1$ and $-\phi_1 < \phi_2$. Additionally the sequence is bounded, where the least upper bound is 1. Hence $\lim_{n \rightarrow \infty} x_n = 1$, which means that the characteristics are attracted by the lower right corner.

A case where the starting characteristic is corresponding to ϕ_2 can be put down to the above mentioned case by rotation. Then the characteristics approach the upper left corner. \square

Such a case of limit behavior is called a *subcritical* case (Figure 3(a)). Locating a convenient fundamental interval where the streamfunction can be prescribed is rather simple in such a case and will be discussed in section 3. If $\phi_2 > 0$ the limit behavior becomes more complicated, since back-reflections can annihilate the ordering. Those cases are called *supercritical* cases (Figure 3(b)).

There are three possible types of limit behavior in a supercritical case, namely *periodic*, *ergodic* and *attractor* cases, see [2]. In a periodic case the web $S(x_0)$ consists only of a finite

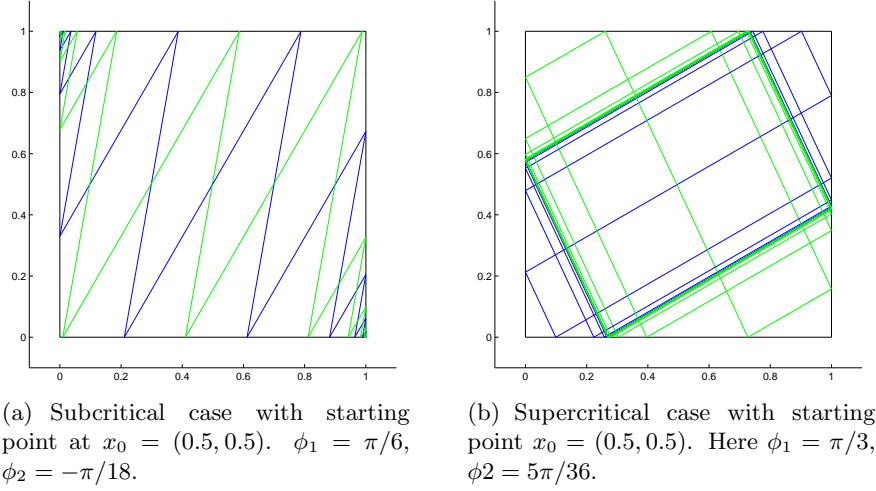


Figure 3: Examples of sub- and supercritical cases.

number of elements, i. e. $S(x_0) = \{x_0, x_1, \dots, x_n\}$ with a fixed n for any x_0 . If for each x_0 the trajectory comes arbitrary close to any point in the square, the case is called ergodic or quasi-periodic. The most frequently occurring case of limit behavior is the attractor. In this case the characteristics are attracted towards a limit cycle. For our geometry the occurring attractors are always global attractors, i. e. for any starting point the characteristics get attracted towards the same limit cycle. Attractors are characterized by the number of boundary intersections they have. The overall number of an attractor's intersections with the boundary is called the attractor's period. Due to the symmetry it is sufficient to count only the intersections on the left and top of the boundary. An attractor with m intersections at the left and n intersections at the top is referred to as an (m, n) -attractor. The simplest type of attractor is a $(1, 1)$ -attractor, a so-called *simple attractor*. It is remarkable that simple attractors occur in a continuous region of the parameterspace.

Theorem 2. *A simple attractor occurs if and only if $\frac{\pi}{4} < \phi_1 \leq \frac{\pi}{2} - \phi_2$.*

Proof. It is clear that the possibility to inscribe a parallelogram inside the square is a necessary condition for the occurrence of a simple attractor. From the figure below we observe the following conditions.

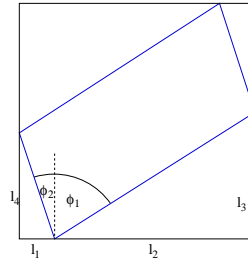
$$l_1, l_2, l_3, l_4 > 0, \quad (4)$$

$$1 = l_1 + l_2, \quad (5)$$

$$1 = l_3 + l_4, \quad (6)$$

$$l_1 = t_2 l_4, \quad (7)$$

$$l_2 = t_1 l_3 \quad (8)$$



Adding up (7) and (8) in consideration of (5) and (6) yields

$$1 = l_4(t_2 - t_1) + t_1.$$

and hence

$$l_4 = \frac{t_1 - 1}{t_1 - t_2}$$

Since $l_4 > 0$ by assumption it follows that $\phi_1 > \frac{\pi}{4}$.

Now, let $\frac{\pi}{4} < \phi_1 \leq \frac{\pi}{2}$. Since $\phi_1 > \frac{\pi}{4}$ the positive-slope characteristics have a slope smaller than 1, which implies that for any starting point at the bottom the next intersection point will be at the right. Additionally we have $\phi_2 \leq \frac{\pi}{2} - \phi_1 < \frac{\pi}{4}$ and hence the negative-slope characteristics have a slope smaller than -1 . This means that for any starting point on the right the next intersection point will be on the top. Altogether we can compute a map which maps a point at the bottom again to the bottom, independent of the points position. This map is given by

$$T(x) = (t_2^2/t_1^2)x + c,$$

with a constant

$$c = t_2 \left(1 - 1/t_1 + t_2/t_1 - t_2/t_1^2 \right),$$

Due to the assumptions

$$T'(x) = t_2^2/t_1^2 < 1$$

holds true and so the sequence of successive iterations $x_{n+1} = T(x_n)$ converges towards the unique fixed point x_* of T , where

$$x_* = \frac{t_2(1/t_1 - 1)}{t_2/t_1 - 1}$$

The fact that $T(x) \neq x$ for almost all x additionally implies that there is no possibility for periodic behavior in this case. \square

In particular this means that for $\phi_1 > \frac{\pi}{4}$ and $\phi_2 \leq \phi_1 - \frac{\pi}{4}$ the only occurring limit behavior in a supercritical case is the approach to a simple attractor. In terms of the tilted square with tilt angle θ this is the case for $\frac{\pi}{8} \leq \theta \leq \frac{3\pi}{8}$.

Now we have characterized three quarters of the parameterspace. The limit behavior in the remaining quarter is more complex. In this region all possible types of limit behavior occur, particularly high period attractors. Figure 4 shows the distribution of these attractors in the corresponding region of parameterspace.

Now we are going to characterize periodic cases with help of the critical characteristics.

Theorem 3. *Periodic orbits for each starting point occur if and only if each corner gets mapped to another.*

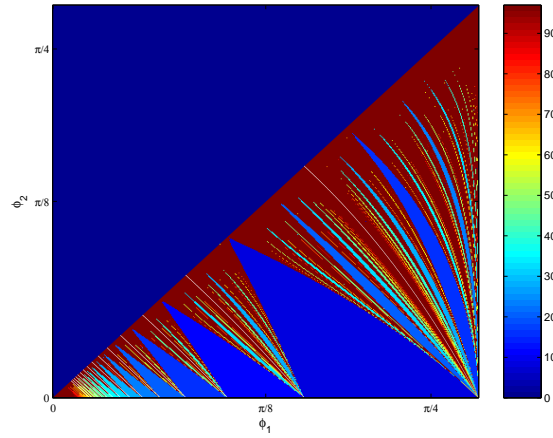


Figure 4: For each pair (ϕ_1, ϕ_2) the period of the corresponding attractor is plotted. The dark red areas represent attractors with period ≥ 100 . The white lines indicate periodic cases, see below. Notice that the upper left part is not a part of the restricted parameterspace.

Proof. If every starting point gets mapped to itself after a finite number of iterations particularly a corner point has to get mapped to itself. But the only possibility for this is to map a corner to another and to go the same way back.

Now we presume that every corner gets mapped to another. If the characteristics were approaching an attractor also the critical characteristics would have to approach this attractor. Since this is not possible and obviously such a case cannot be an ergodic one this must be a periodic case. \square

This characterization of periodic cases in principle allows us to compute the parameters (ϕ_1, ϕ_2) for which periodic cases occur analytically. As an example we consider the case where a characteristic starting at the lower left corner of the square intersects the lower right corner after $2k$ successive intersections at the top and bottom. With the help of simple analysis, we obtain that the relation between ϕ_1 and ϕ_2 in such a case, is given by the nonlinear equation

$$k(t_1 + t_2) = 1,$$

and finally we get

$$\phi_2 = \arctan(1/k - t_1).$$

The contribution of these periodic cases for $k = 1, \dots, 15$ within the upper left part of the restricted parameterspace is depicted in Figure 5. Additionally you can see this contribution in Figure 4, where these periodic cases are indicated by the white lines. For more complicated types of periodicity the analytic computation becomes too complex. But the above mentioned procedure can be used to obtain numerical results.

Another way to get an impression of the limit behavior is to look at a Poincaré plot. At this the positions of the last few hundred intersection points on the left boundary as well

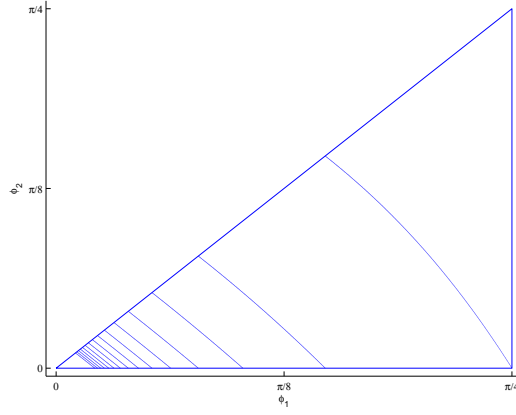


Figure 5: Here the pairs (ϕ_1, ϕ_2) for which the explained type of periodic case occur are plotted for $k = 1, \dots, 15$.

as the top boundary are plotted after performing a large number of iterations. Here this is done for a fixed tilt angle $\theta = (\phi_1 - \phi_2)/2$ as $\phi = (\phi_1 + \phi_2)/2$ varies from θ to $\pi/4$. Such a plot is given by Figure 6, where $\theta = \pi/18$. For each gridpoint there have been 7500 iterations performed, where only the last 500 are plotted. The upper subplot depicts the intersections on the left boundary, the lower one those on the top boundary. The figure shows regions where the attractor period is constant, separated by regions with high period attractors. We already know that simple attractors only occur in that part of the restricted parameterspace where $\phi_1 > \pi/4$. Here this means that ϕ has to be larger than $35\pi/180$ as can be clearly observed in the plot. Examination of the windows where no attractors are visible at a finer scale, shows a form of self-repeating structure, where these regions are again divided in windows showing attractors with a relative small period and other windows with high period, which is shown in Figure 7. This figure also shows that the attractor period increases rapidly while approaching a periodic case at $\phi \approx 257\pi/1800$.

A third possibility to study the limit behavior is with the help of the rotation number. The rotation number is defined by

$$\rho = \lim_{n \rightarrow \infty} \frac{\tilde{T}^n(x_0)}{n}.$$

Here the map $T = c^{-1} \circ F \circ c$ is the composition of a function $F : \partial S \rightarrow \partial S$ which returns the next but one boundary intersection point and a parameterization of the boundary $c : \partial S \rightarrow [0, 4[$. For more information on T see Appendix A. $\tilde{T} : \mathbb{R} \rightarrow \mathbb{R}$ is a continuous transformation of T which is uniquely determined up to addition of a constant integer. It can be shown that the rotation number is independent of the starting point x_0 . Interesting about the rotation number is, that a rational rotation number corresponds to either an attractor or periodic case and a irrational rotation number corresponds to an ergodic case. If ρ is a rational number, and additionally $T^n = I$ for some $n \in \mathbb{N}$, then T is periodic, otherwise attractive. Besides that the rotation number varies continuously and monotonously with

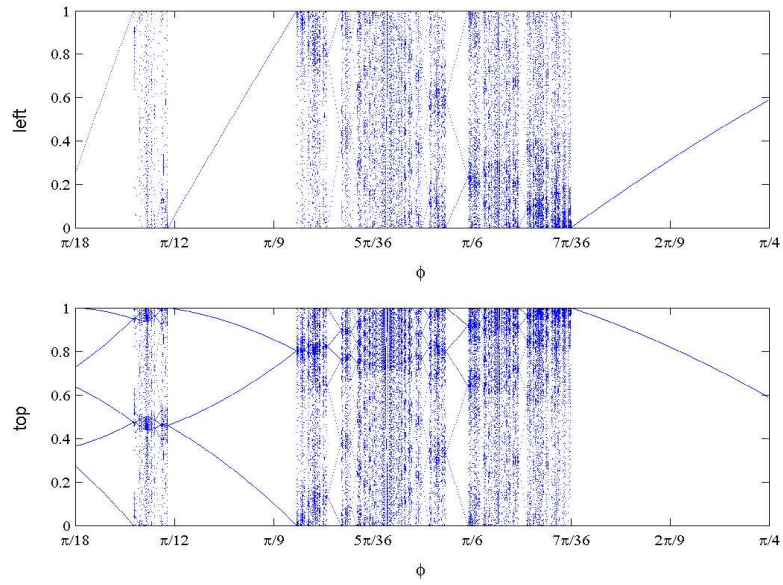


Figure 6: Poincaré plot for $\theta = \pi/18$. The last 500 intersection points after 7500 iterations are plotted.

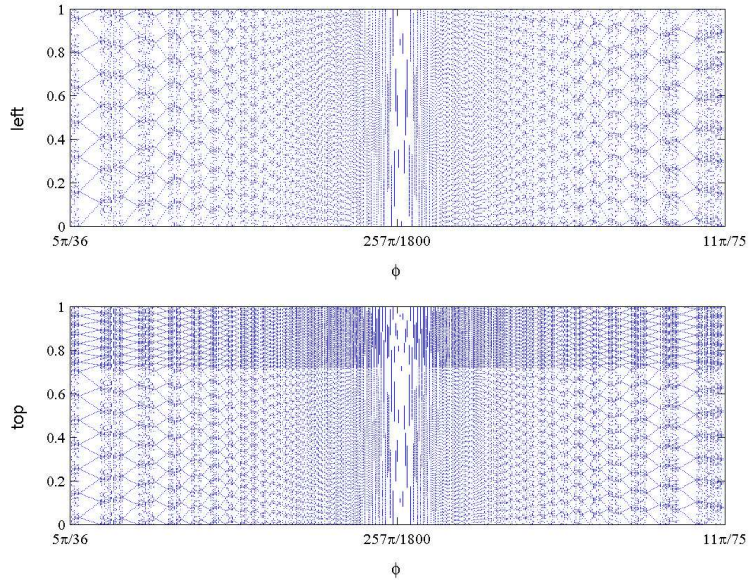
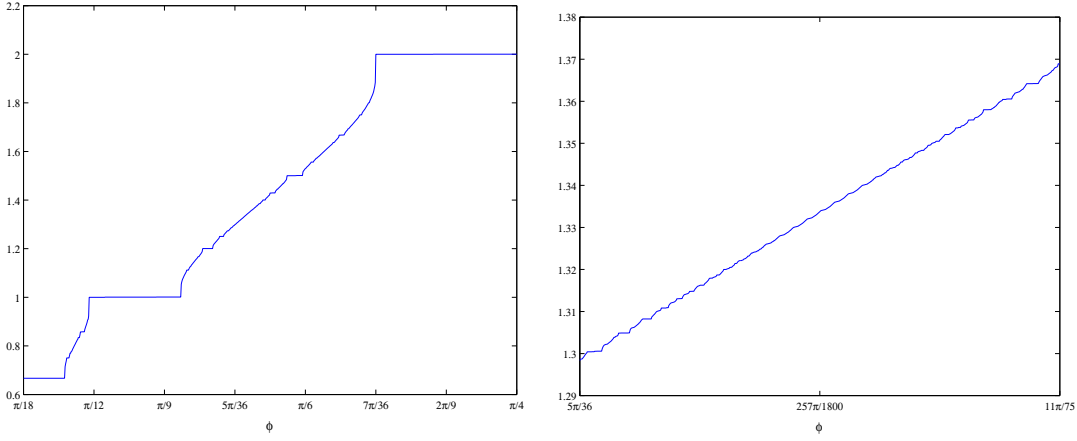


Figure 7: Examination of Figure 6



(a) Rotation number for fixed tilt angle $\theta = \pi/18$.

(b) Examination of Figure 8(a).

Figure 8:

the parameters ϕ_1, ϕ_2 and remains constant in the attractive areas of the parameterspace. This behavior can be clearly observed by Figure 8(a) and Figure 8(b). Comparing these two figures with the Poincaré plots from above, we can see identical behavior for the different parameter values.

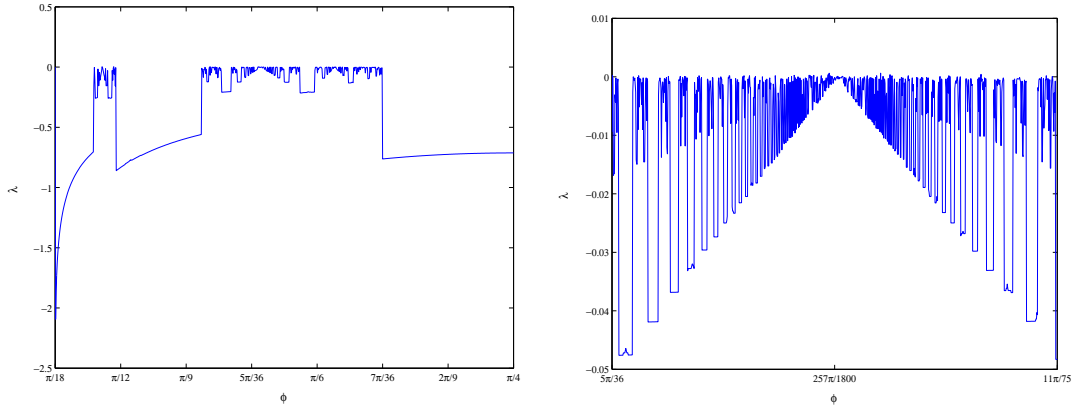
Although one might expect, there is no chaotic behavior within the high period windows. One way to obtain this result is the computation of Lyapunov exponents

$$\lambda = \lim_{n \rightarrow \infty} \frac{1}{N} \sum_{n=0}^{N-1} \log \left| \frac{dT_n}{dx}(x_0) \right|.$$

The Lyapunov exponent measures the overall convergence or divergence of nearby characteristics. At this chaos is associated with $\lambda > 0$. Although the Lyapunov exponent is a function of x_0 the same λ will be obtained for almost any starting point x_0 . Figure 9(a) shows the Lyapunov exponents for fixed tilt angle $\theta = \pi/18$. Comparing it with figure 6 we can observe relative small Lyapunov exponents in the windows with small attractor periods and Lyapunov exponents close to zero in the regions with high period attractors and ergodic cases. At this a Lyapunov exponent $\lambda = 0$ either indicates a periodic or ergodic case. Anyway, no positive Lyapunov exponents can be observed. Figure 9(b) is corresponding to the Poincaré plot figure 7 and also mimics this plot.

3 Computation of the streamfunction

As mentioned before we can compute the streamfunction field by prescribing the function F on appropriate intervals at the boundary. Thereby it turns out that at most two intervals are enough. In subcritical cases it suffices to prescribe F on only one interval. Locating such



(a) Lyapunov exponents corresponding to Figure 6 (b) Examination of Figure 9(a) corresponding to Figure 7

Figure 9:

an interval is rather simple. For instance we can choose any interval $[x_n, x_{n+1}[$ between two successive characteristics intersections x_n and x_{n+1} on the boundary. Having prescribed F on such an interval the function is already prescribed on the whole boundary.

In supercritical cases we have to distinguish between the three types of limit behavior. In an ergodic case there exists only one web. Thus, we can prescribe the solution only in one single point at the boundary. Taking the boundary condition (2) into account yields that the solution is the trivial solution $\psi = 0$. In order to locate appropriate intervals for periodic and attractor cases we used the following Algorithm 1, see Appendix B. In case of a simple attractor a proper choice of intervals are the ones depicted in Figure 10. One can quite easily assure oneself that these intervals are chosen right. Algorithm 1 seems to be a consequentially extension of the way to choose the intervals in case of a simple attractor, but it would be much nicer if this could be proved.

Having determined the position of appropriate intervals where F can be prescribed, it is an easy task to compute the streamfunction field $\psi = F - G$. We also can compute the pressure field which is given by $p = F + G$. The following examples of streamfunction and pressure fields, where computed by prescribing two cosines with an offset at the chosen intervals. Figure 11 shows the streamfunction and pressure field in case of a simple attractor. Here $\phi_1 = \pi/3$ and $\phi_2 = 5\pi/36$ corresponding to Figure 3(b). We observe a self repeating structure near the attractor in both subplots. Figure 12 depicts the streamfunction field and pressure field for $\phi_1 = \pi/6$ and $\phi_2 = \pi/18$. This means that $\theta = \pi/18$ and $\phi = \pi/9$. A more complex attractor and the corresponding streamfunction and pressure field is shown by Figure 13. Here $\phi_1 = \pi/6$ and $\phi_2 = 13\pi/180$. In a periodic case, for example with $\phi_1 = \pi/6$ and $\phi_2 = \arctan(1 - t_1)$ we obtain smooth streamfunction and pressure fields. This is due to the fact that in this cases the web of a point x_0 divides the boundary into a finite number of distinct intervals. Of course one has to prescribe a smooth function at boundary, in order

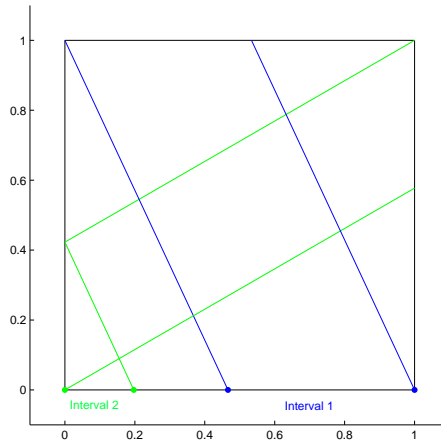


Figure 10: Appropriate choice of intervals in case of a simple attractor

to obtain smooth streamfunction and pressurefields. See Figure 14.

4 Discussion

A still open question is for which parameters ergodic cases occur, or if these cases occur at all. Figure 4 and Figure 7 suggest, that periodic cases appear at the heart of regions with high period attractors. But this leaves little room for the ergodic cases. Candidates for ergodic cases could be the boundaries between regions with high and low period attractors, but this has not been further examined yet. One way to answer this question would be the analytically computation of rotation numbers, but this seems to be quite a hard task.

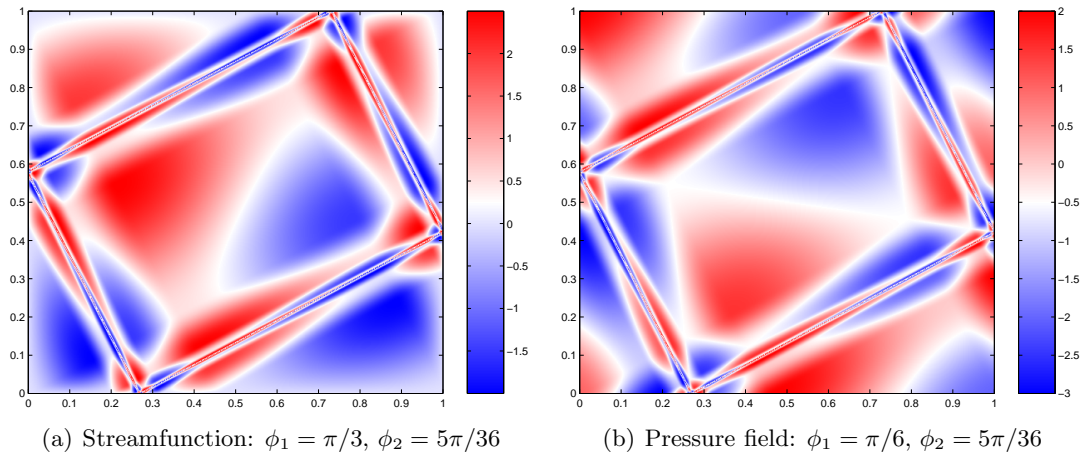


Figure 11:

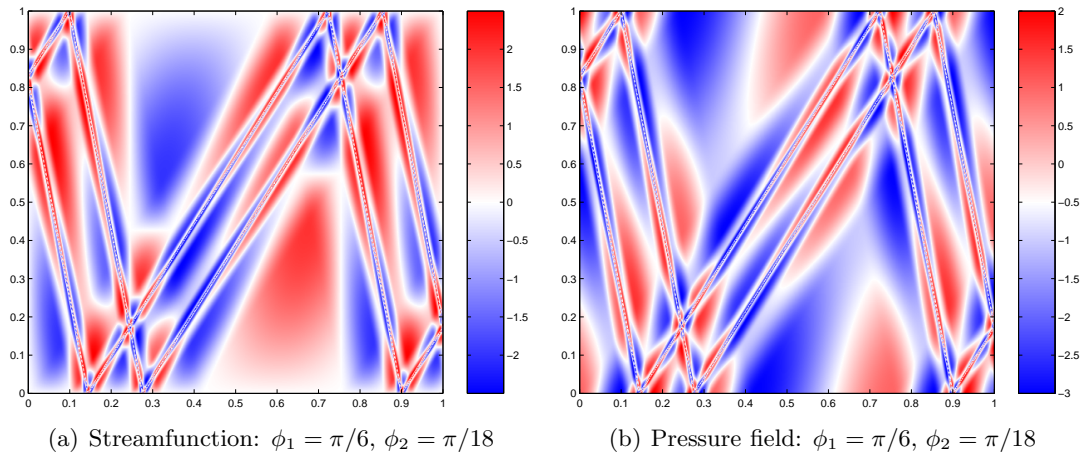


Figure 12:

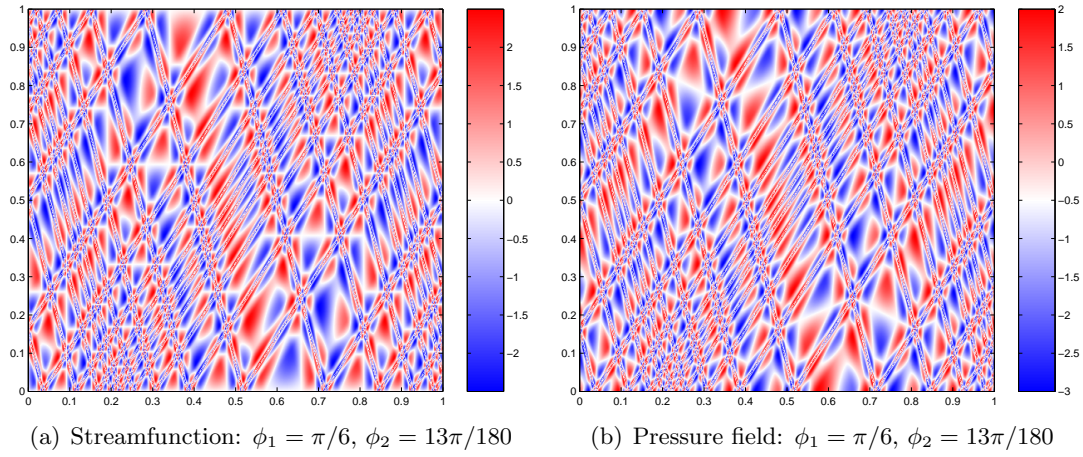


Figure 13:

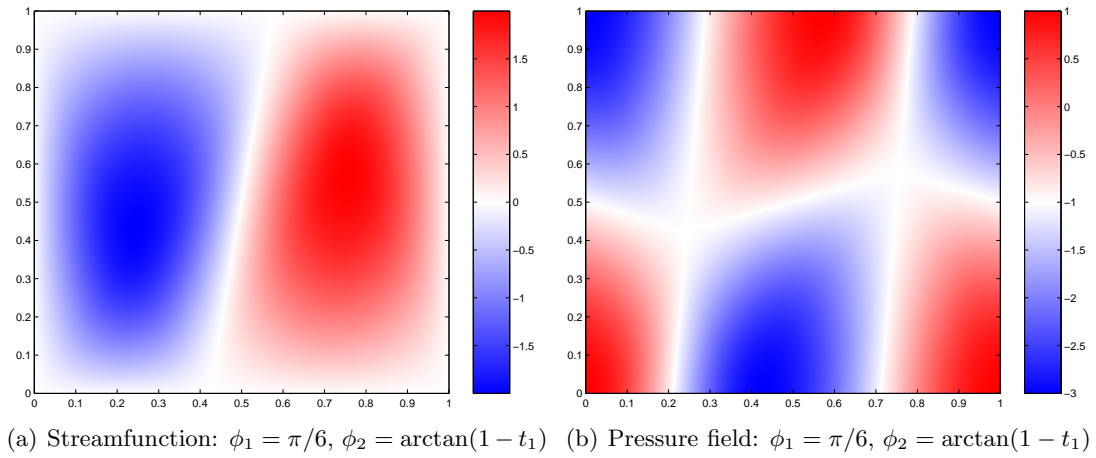


Figure 14:

A Analytic map

In order to get a more analytic approach to the characteristics limit behavior we can compute a map $F : \partial S \rightarrow \partial S$ of the circumference to itself. Combining two successive intersections as one, we obtain an orientation preserving map, where F can be represented as $F = T^- \circ T^+$. At this $T^- : \partial S \rightarrow \partial S$ is defined by

$$T^-(x, y) = \begin{cases} (0, x/t_2), & 0 \leq x \leq x^*, y = 0, \\ (x - t_2, 1), & x^* < x \leq 1, y = 0, \\ (1 + t_2(y - 1), 1), & x = 1, \\ (x + t_2, 0), & 0 \leq x \leq x^{**}, y = 1, \\ (1, 1 - (1 - x)/t_2), & x^{**} \leq x \leq 1, y = 1, \\ (yt_2, 0), & x = 0, \end{cases}$$

$$x^* = t_2, \quad x^{**} = 1 - t_2,$$

and returns the next intersection point along the negative characteristics. Similarly $T^+ : \partial S \rightarrow \partial S$ returns the next intersection point along the positive characteristics and is given by

$$T^+(x, y) = \begin{cases} (x + t_1, 1), & 0 \leq x \leq x^*, y = 0, \\ (1, (1 - x)/t_1), & x^* < x \leq 1, y = 0, \\ (1 - yt_1, 0), & x = 1, \\ (0, 1 - x/t_1), & 0 \leq x \leq x^{**}, y = 1, \\ (x - t_1, 0), & x^{**} \leq x \leq 1, y = 1, \\ ((1 - y)t_1, 1), & x = 0 \end{cases}$$

$$x^* = 1 - t_1, \quad x^{**} = t_1$$

if $\phi_1 < \frac{\pi}{4}$ and by

$$T^+(x, y) = \begin{cases} (1, (1 - x)/t_1), & y = 0, \\ (1 - yt_1, 0), & 0 \leq y \leq y^*, x = 1, \\ (0, y - 1/t_1), & y^* < y \leq 1, x = 1, \\ (0, 1 - x/t_1), & y = 1, \\ (1, y + 1/t_1), & 0 \leq y \leq y^{**}, x = 0, \\ ((1 - y)t_1, 1), & y^{**} < y \leq 1, x = 0 \end{cases}$$

$$y^* = 1/t_1, \quad y^{**} = 1 - 1/t_1$$

if $\phi_1 > \frac{\pi}{4}$.

A parameterization of the boundary ∂S is for instance given by $c : [0, 4[\rightarrow \partial S$,

$$c(t) = \begin{cases} (t, 0), & 0 \leq t \leq 1, \\ (1, t - 1), & 1 < t \leq 2, \\ (3 - t, 1), & 2 < t \leq 3, \\ (0, 4 - t), & 3 < t < 4 \end{cases}$$

with inverse function $c^{-1} : \partial S \rightarrow [0, 4[$,

$$c^{-1}(x, y) = \begin{cases} x, & y = 0, \\ y + 1, & x = 1, \\ 3 - x, & y = 1, \\ 4 - y, & x = 0. \end{cases}$$

The map $T : [0, 4[\rightarrow [0, 4[$ which was used to compute the Lyapunov exponents in section 2.2 is the composition $T = c^{-1} \circ F \circ c$.

B Algorithm for computing intervals where the streamfunction can be prescribed

Algorithm 1 Interval algorithm

▷ The square's corners are denoted counterclockwise by A, B, C, D, starting with the lower left corner.

$a_2 \leftarrow 0, b_1 \leftarrow 1$

for each of the corners A, B, C, D **do**

 compute the web $S(c) = \{x_0^c, x_1^c, x_2^c, \dots\}$,

 extract the subsequence $\{x_{n_i}^c\}$ of bottom-intersections

end for

$b \leftarrow \min\{x_{n_i}^C\}, b^* \leftarrow \min\{x_{n_i}^B\}$

if $\min(b, b^*) = 0$ **then**

$b_2 \leftarrow \max(b, b^*)$

else

$b_2 \leftarrow \min(b, b^*)$

end if

$a \leftarrow \max\{x_{n_i}^A\}, a^* \leftarrow \max\{x_{n_i}^D\}$

if $a = a^*$ **then**

$a_1 \leftarrow 1$

else

$a_1 \leftarrow \max(a, a^*)$

end if

$I_1 \leftarrow [a_1, b_1], I_2 \leftarrow [a_2, b_2]$

if $|I_1| = 0$ **then**

$I_1 \leftarrow \emptyset$

else if $|I_2| = 0$ **then**

$I_2 \leftarrow \emptyset$

end if

return I_1, I_2

References

- [1] L. Maas, F.-P. Lam; *Geometric focusing of internal waves*; J. Fluid Mech. (1995); vol. 300; pp. 1-41
- [2] A. Swart, G. Sleijpen, L. Maas, J. Brandts; *Numerical solution of the two dimensional Poincaré equation*; preprint; (publication in J. Comp. Appl. Math. (2006))
- [3] F. John; *The Dirichlet problem for a hyperbolic equation*; Am. J. Math (1941); vol. 63; pp. 141-154